From a One-Legged Verical Jump to the Speed-Skating Push-off: A Stimulation Study

Bobbert, M.F.; Houdijk, J.H.P.; de Koning, J.J.; de Groot, G.

published in
Journal of Applied Biomechanics
2002

DOI (link to publisher)
10.1123/jab.18.1.28

document version
Publisher's PDF, also known as Version of record

JOURNAL OF APPLIED BIOMECHANICS, 2002, **18**, 28-45

From a One-Legged Vertical Jump to the Speed-Skating Push-off: A Simulation Study

Maarten F. Bobbert, Han Houdijk, Jos J. de Koning, and Gert de Groot
Vrije Universiteit, Amsterdam

To gain a better understanding of push-off mechanics in speed skating, forward simulations were performed with a model comprising four body segments and six muscles. We started with a simulated maximum height one-legged jump, obtained by optimization of muscle stimulation time histories. The simulated jump was very similar to one-legged jumps produced by a human, indicating that the model was realistic. We subsequently studied how performance was affected by introducing four conditions characteristic of speed skating: (a) We changed the initial position from that in jumping to that at the start of the push-off phase in skating. This change was accommodated by a delay in stimulation onset of the plantar flexors in the optimal solution. (b) The friction between foot and ground was reduced to zero. As a result, maximum jump height decreased by 1.2 cm and performance became more sensitive to errors in muscle stimulation. The reason is that without surface friction, the foot had to be prevented from slipping away, which constrained the solution space and reduced the tolerance to errors in stimulation. (c) We introduced the requirement to maintain the upper body in a more or less horizontal position. This change could be accommodated by a delay in stimulation onset of the hamstrings, which inevitably caused a reduction in maximum jump height by 11.6 cm. (d) We increased the effective foot length from 16.5 cm, representative of jumping, to 20.5 cm, representative of skating with klapskates. At the 20.5-cm foot length, rotation of the foot did not start during the buildup of plantar flexion moment as it did at smaller foot lengths, but was delayed until hip and knee extension moments decreased. This caused an unbalanced increase in segment angular velocities and muscle shortening velocities, leading to a decrease in muscle force and muscle work and a further decrease in maximum jump height by approximately 5 cm. Qualitatively, these findings help clarify why and how performance of speed skaters depends on the location of the hinge of their skate.

Key Words: human, musculoskeletal model, biomechanics, optimal control

---

The authors are with the Institute for Fundamental and Clinical Human Movement Sciences, Vrije Universiteit, Van der Boechorststraat 9, 1081 BT Amsterdam, The Netherlands.

Introduction

Speed skating is a peculiar form of locomotion. The push-off during skating may be compared to a one-legged jump executed while falling sideways (de Boer, Cabri, Vaes, et al., 1987). The reaction force generated during the push-off is always perpendicular to the gliding direction of the skate, because ice friction along the blade is negligible. The force has a forward component because the skater is tilted in the frontal plane while the skate is not gliding in the direction of the track but at an angle to it (Allinger & van den Bogert, 1997).

Since the push-off occurs while the skate is gliding forward over the ice, top skaters can achieve steady-state speeds of over 12 m/s during a 10-km race. This is about twice the speed achieved by runners in a 10-km running competition. Nevertheless, the push-off in speed skating is constrained compared to that in jumping (de Boer et al., 1987; van Ingen Schenau, 1989). The upper body is held more or less horizontal during skating to minimize the frontal area and thereby the loss of energy due to air friction (van Ingen Schenau, 1982). Moreover, when skating with conventional skates, in which the shoe is fixed rigidly to the blade, rotation of the foot (plantar flexion) is suppressed, or so it was argued, to prevent the tip of the skate from scratching the ice; such scratching would cause an increase in the amount of work required in overcoming ice friction (van Ingen Schenau & Bakker, 1980).

Suppression of foot rotation limits the work output at the ankle and requires a coordination pattern that differs from the pattern observed in natural forms of locomotion such as running and jumping. To allow skaters to rotate their foot more naturally during the push-off and produce more work with their plantar flexors, without a concomitant increase in ice friction, a skate was invented with a hinge joint between the shoe and the blade: the klapskate (van Ingen Schenau, Bobbert, & Rozendal, 1987; van Ingen Schenau, de Groot, Scheurs, Meester, & de Koning, 1996).

When the world's top speed skaters adopted the klapskate in the 1997–98 season, world record times for the Olympic distances improved an average of 2.9% for men and 2.5% for women (Allinger & Motl, 2000). Does this mean the ideas that led to the development of the klapskate were correct? In search of an answer to this question, a kinematic and kinetic intraindividual comparison was made between skating with klapskates and skating with conventional skates (Houdijk, de Koning, de Groot, Bobbert, & van Ingen Schenau, 2000). The higher speed with klapskates, and the underlying higher mean power output, turned out to be due partly to a higher stroke frequency and partly to a greater amount of total work per stroke. Contrary to expectations, however, the greater work per stroke on klapskates was not due to a greater work output at the ankle but instead to a greater work output at the knee joints. Apparently our understanding of the mechanics of the push-off in speed skating, and the effects of construction of the skate, was incomplete.

So far there have been attempts to gain insight into the push-off mechanics in skating by taking measurements during skating (e.g., Houdijk et al., 2000; Houdijk, de Koning, Bobbert, & de Groot, 2001) or during vertical jumps executed by skaters (Allinger & Motl, 2000). Unfortunately, such measurements yield noisy data, and important variables such as individual muscle forces cannot be measured. Moreover, the experimenters cannot fully control what a skater does,

nor manipulate properties of the skater such as maximal muscle forces. These drawbacks do not apply to forward simulations with an optimal control model. Allinger and van den Bogert (1997) developed a model to determine the optimal skating technique. However, their model uses leg length as a function of time as input and does not allow for an analysis of the work output at the joints and the contributions of individual muscles. Models that do permit such an analysis have been successfully developed for vertical jumping (Pandy, Zajac, Sim, & Levine, 1990; van Soest, Schwab, Bobbert, & van Ingen Schenau, 1993). Such models can perhaps be applied to speed skating, considering that, as argued above, the push-off during skating can be compared to that of a one-legged jump with constrained upper body and foot rotation.

The purpose of the present study was to gain a better understanding of the mechanics of the push-off in speed skating with the help of an optimal control model developed for jumping. Starting from a simulated maximum height one-legged jump, we studied how performance was affected by implementing in the model four characteristics that distinguish speed skating from jumping: (a) the starting position was changed from that in jumping to that in speed skating; (b) the friction between foot and ground was reduced to zero; (c) the requirement to maintain the upper body in a more or less horizontal position was introduced; and (d) the effective foot length was increased from natural values to values operative in speed skating. Simulation results were compared to experimental results on one-legged jumping and speed skating.

Methods

To determine initial conditions for simulations and to evaluate simulation results, we used kinematic and kinetic data obtained from a male good jumper (mass 70 kg, height 1.83 m) performing one-legged vertical squat jumps, as well as data from a Dutch elite skater (mass 83 kg, height 1.80 m) skating 400-m laps at a speed of 10 m/s on klapskates. The jumping data were collected as part of the present study. Informed consent was obtained from the participant in accordance with the policy statement of the American College of Sports Medicine. The participant performed 10 maximum effort one-legged jumps and the highest was used for presentation purposes. The speed skating data were collected in a study on Dutch sprint elite skaters, described elsewhere (Houdijk et al., 2001). The skater and trial selected for presentation were representative of the group of skaters participating in that study.

The locations of markers representing neck, hip joint, knee joint, ankle joint, and 5th metatarso-phalangeal joint and, in skating, the blade of the skate, were acquired using an OptoTrak 3020 motion registration system (Northern Digital Inc., Waterloo, Ontario) operating at 180 Hz. Ground reaction forces produced during jumping were measured using a Kistler force platform (type 9281B, Kistler Instrument Corp., Amherst, NY) and sampled simultaneously with the kinematic data at 180 Hz. Ground reaction forces produced during skating were measured using klapskates equipped with strain-gauge elements underneath the heel and hinge of the skate (Houdijk et al., 2000; Houdijk et al., 2001), and sampled at 1 kHz by a portable computer. The data collected during jumping were projected on the sagittal plane, while data collected during skating were projected on a moving

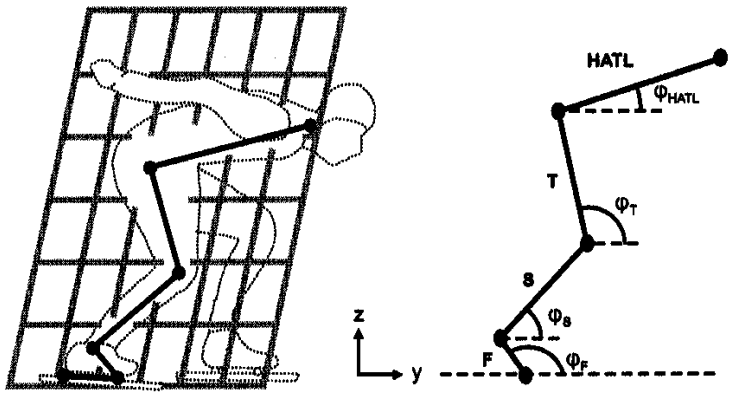

Figure 1 — Locations of anatomical landmarks defining body segments, and definition of segment angles φ relative to the right horizontal. Segments are foot (F), shank (S), and thigh (T) of the push-off leg, and a rigid segment representing head, arms, trunk, and swing leg (HATL). Jumping data were projected on the sagittal plane. Speed skating data were projected on the plane best fitting the landmarks on skate, ankle, knee, and hip joint. The y-axis is the line of intersection between this moving plane and the surface of the ice; the z-axis is oriented perpendicular to the y-axis and runs through the hip joint. It was assumed that the reaction force vector lay in this y–z reference plane.

reference plane through landmarks on the skate, ankle, knee, and hip joints (Figure 1). All data were low-pass filtered at 15 Hz.

For the simulations, we used a two-dimensional forward dynamic simulation model of the human musculoskeletal system (Figure 2). The model, which calculates the motion of body segments corresponding to muscle stimulation-time input, has been described in detail elsewhere (van Soest et al., 1993). For the present study it was modified to consist of three rigid segments representing foot, shank, and thigh of the push-off leg, and a fourth rigid HATL segment representing head, arms, trunk, and swing leg (henceforth, the term *leg* refers to the whole lower extremity). No passive constraints on joint ranges of motion were included.

In the skeletal submodel of the push-off leg, six major muscle-tendon complexes (MTCs) were embedded. They were (with maximum isometric forces in parentheses): soleus (4000 N), gastrocnemius (2000 N), vasti (4500 N), rectus femoris (1500 N), gluteus maximus (2500 N), and hamstrings (2000 N). Each of these MTCs was represented by a Hill-type muscle model consisting of a contractile element (CE), a series elastic element, and a parallel elastic element (van Soest & Bobbert, 1993; van Zandwijk, Bobbert, Baan, & Huijing, 1996). Contraction velocity of CE depended on active state, CE length, and force. The maximum shortening velocity of all muscles was 12.7 times muscle fiber optimum length per second. Active state, the relative amount of Ca^{++} bound to troponin, was calculated using a saturating trend function from the free Ca^{++} concentration (Hatze,

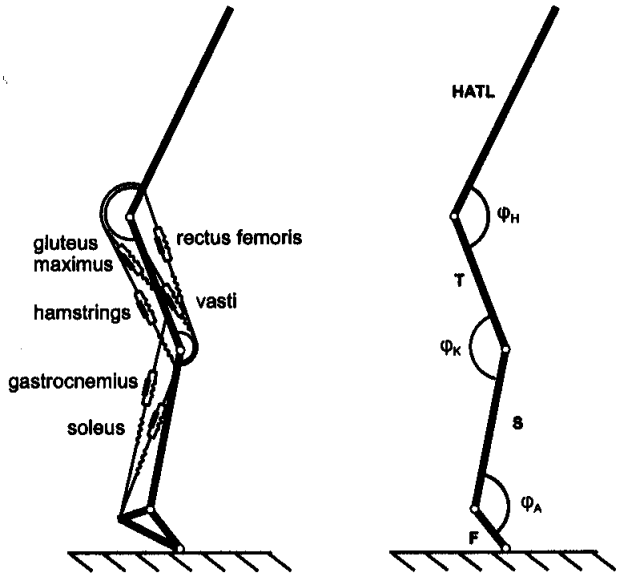

Figure 2 — Schematic of the musculoskeletal system model used for forward dynamic simulations. The model consists of four interconnected rigid segments (cf. Figure 1) and six muscle groups of the lower extremity, all represented by Hill-type muscle models. Diagram at right shows the definition of angles φ at the ankle (A), knee (K), and hip (H) joint.

1981). This latter concentration, in turn, changed with muscle stimulation STIM according to a first-order differential equation (Hatze, 1981, pp. 31-42). STIM, ranging between 0 and 1, was a one-dimensional representation of the effects of recruitment and firing frequency of α-motoneurons.

To set the parameters of the HATL segment, we used the body configuration observed at the start of the push-off in the jumper (Figure 3a) and the one at the end of the gliding phase in the speed skater (Figure 3c). In jumping, effective foot length was defined as the shortest distance between the axis of rotation of the ankle joint and the 5th metatarso-phalangeal joint. This distance was 16.5 cm. In skating, it was defined as the shortest distance between the axis of rotation of the ankle joint and the axis of rotation of the skate (in klapskating, the hinge between the shoe and the blade; in conventional skating, the tip of the blade). A change in the location of the klapskate's axis of rotation was modeled by changing the foot length and, at the same time, (a) adjusting the initial foot angle to ensure that the height of the ankle joint remained the same, and (b) adjusting the rest length of series elastic elements of gastrocnemius and soleus so that the initial CE lengths of these muscles remained the same.

For each condition to be studied, we had to formulate a dynamic optimization problem. The following restrictions were imposed on STIM: first, initial STIM-levels of soleus, vasti, and gluteus maximus were set in such a way that

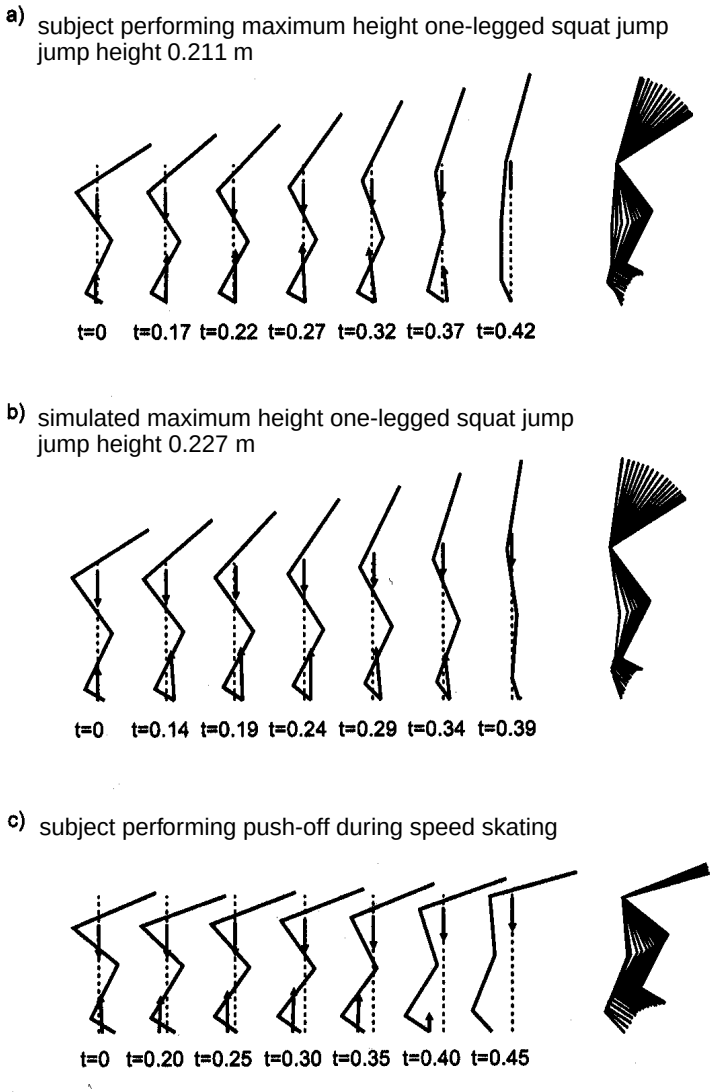

Figure 3 — Experimental data for the push-off in maximum height one-legged squat jumping from the preferred initial position (a), a simulated maximum height one-legged jump (b), as well as experimental data for the push-off in skating with klapskates (c). Panels (a) and (c) represent different participants. In each panel, the leftmost stick figure shows the position at the start of upward motion of the center of mass, the rightmost one shows the configuration at the last frame before the push-off leg lost contact with the ground. The intermediate diagrams are spaced 50 ms in time, starting at the instant of takeoff and counting back in time. In each stick figure, the ground reaction force vector is represented with its origin at the center of pressure, and the force of gravity is shown with its origin at the center of mass. Dotted line represents stationary environment in (a) and (b), and horizontal position of the center of mass in (c). In the rightmost column, the configurations of the system were plotted at 20-ms time intervals with the hip joint used as origin.

static equilibrium was achieved in the initial position. Second, STIM of each muscle was allowed to either keep this initial value or take on its maximal value. For simulation of the jump to be used for evaluation of the model, this maximal value was set at 1.0. For all other simulations it was lowered to 0.5, in an attempt to account for the fact that the skater was skating 400-m laps rather than performing one single maximal push-off. Third, STIM was allowed to switch to the maximum value just once, and thereafter had to keep this value until takeoff. The optimization problem was thus reduced to finding the combination of six switching times that produced the maximum value of the optimization criterion.

For maximum height one-legged jumping with and without surface friction, we selected as the optimization criterion the height attained by the center of mass. The requirement of maintaining the upper body in a more or less horizontal position was introduced by changing the optimization criterion: from jump height we subtracted a penalty value representing the deviation of HATL angle from the initial angle. (Based on pilot work, the penalty was set to 20 times the squared difference between initial HATL angle and HATL angle at takeoff.) The optimization problems were solved using a genetic algorithm (van Soest & Casius, in press). For each condition, the optimization ran for 4,000 generations of a population of 100 chromosomes, with each chromosome being a bit-string, coding a combination of six stimulation onset times.

The optimal solutions of the simulated tasks were compared in terms of jump height (expressed as the difference between height of the center of mass at the apex of the jump and height when standing upright), muscle stimulation onset times, kinematics and kinetics, work contributions of individual muscles, and sensitivity of performance to small perturbations of optimal stimulation onset times of the muscles. This latter sensitivity was determined by simulating 400 jumps in which the optimal muscle stimulation onset times were perturbed. The perturbation was accomplished by adding to each onset time a number taken from a Gaussian-distributed set of pseudo-random numbers with a standard deviation of 2 ms. The smaller the standard deviation of the distribution of heights achieved in these perturbed jumps, the greater the robustness of performance. Finally, the transfer from muscle forces to acceleration of the center of mass and acceleration of the foot was determined using a method similar to that described by Zajac and Gordon (1989).

Results

The maximum one-legged squat jump of the model, obtained by optimization of stimulation onset times (Figure 3b), was very similar to that of the human participant (Figure 3a). The jump height of the model, 22.7 cm, was 1.6 cm greater than that of the participant. From these findings we concluded that the model represented the salient characteristics of the real system. To reduce the intensity of effort in the simulated jump, we lowered the maximum stimulation level from 1.0 to 0.5 and reoptimized stimulation onset times. The resulting movement pattern (Figure 4a) was very similar to that of the maximal jump (Figure 3b). However, the push-off was prolonged by 110 ms and jump height was reduced by 1.7 cm.

In this study we focused on four differences between the push-off in one-legged squat jumping (Figure 3a) and the push-off in speed skating (Figure 3c). First, in skating, the initial position is more crouched and the center of pressure is located more backward relative to the toe. Second, in jumping, the acceleration of

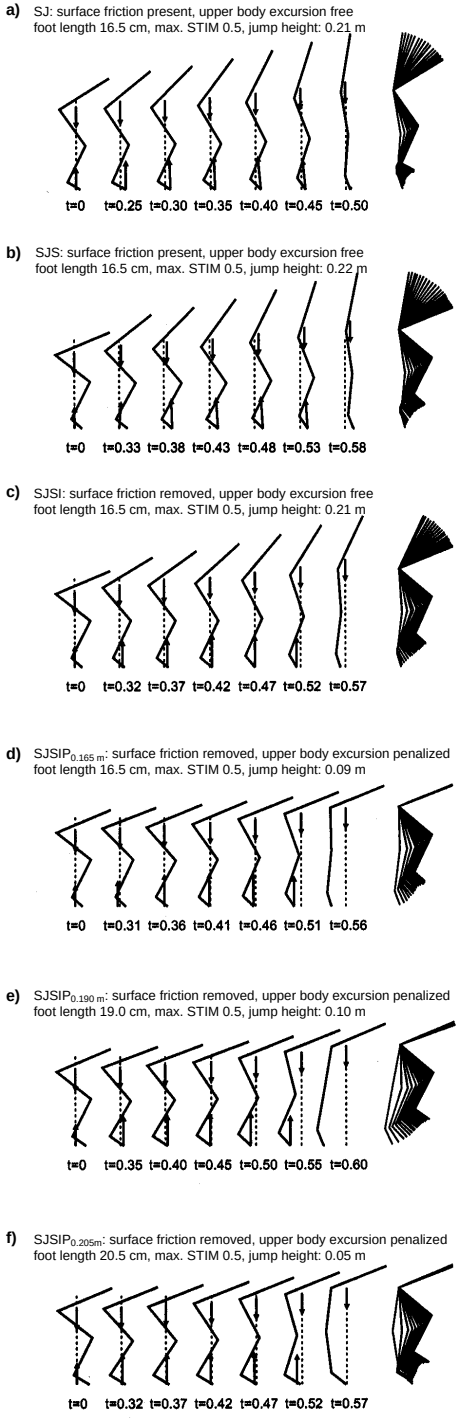

Figure 4 — Optimal solutions for the push-off of the simulation model for different conditions with different optimization criteria. Setup of panels is as in Fig. 3.

(a) SJ: one-legged squat jump from the preferred initial position adopted by jumper (cf. Fig. 3a), with contact friction present, maximum stimulation of 0.5, and an effective foot length of 16.5 cm; optimal stimulation onset times were found using height achieved by center of mass as optimization criterion.

(b) SJS: same condition as SJ, but initiated from the position of the skater at the end of the gliding phase (cf. Fig. 3c).

(c) SJSI: same condition as SJS, but without contact friction.

(d) $SJSIP_{0.165\ m}$: same condition as SJSI, but with a penalty on upper body rotation incorporated in the optimization criterion and an effective foot length of 16.5 cm.

(e) $SJSIP_{0.190\ m}$: same condition as in d, but with a foot length of 19.0 cm.

(f) $SJSIP_{0.205\ m}$: same condition as in d, but with a foot length of 20.5 cm.

Jump height is defined as the height reached by the center of mass at the apex of the jump relative to that in upright standing.

the center of mass has a horizontal component, whereas in skating the foot is accelerated in the gliding direction of the skate, the net outcome being a backward shift of the foot relative to the center of mass. Third, in jumping, the upper body is rotated toward the vertical position, while in skating it is kept more or less horizontal. Fourth, in skating, the distance between the ankle and the center of rotation of the foot is larger than in jumping.

When the initial position of the model was changed to that of the skater at the end of the gliding phase (Figure 4b), this called for changes in the STIM levels of the muscles in order to maintain equilibrium. The initial STIM of gluteus maximus was raised from 0.19 to 0.26. This is noteworthy, because it raised the initial active state of this muscle from 75% to 90%. As a result, the force of gluteus maximus changed very little when it was switched on during the push-off. The change in initial position was accommodated by a change in optimal stimulation onset times: vasti and hip extensors were switched on earlier, and plantar flexors later. From the skater's initial position, the system jumped 22.2 cm high (Table 1).

Table 1 Selected Simulation Results

	t_{SOL} [ms]	t_{GAS} [ms]	t_{VAS} [ms]	t_{REC} [ms]	t_{GLU} [ms]	t_{HAM} [ms]	t_{ho} [ms]	$\varphi_{K,\,ho}$ [rad]	t_{total} [ms]	$z_{CM,max}$ [cm]	$z_{CM,mean}$ [cm]
SJ	0	190	278	364	100	100	280	2.14	500	21.0	21.0 ± 0.1
SJS	321	422	0	412	12	53	440	1.95	580	22.2	22.2 ± 0.0
SJSI	411	161	0	470	156	61	470	2.13	570	21.0	5.7 ± 8.7
$SJSIP_{0.165\ m}$	329	351	84	307	0	222	430	1.97	560	9.4	6.0 ± 3.8
$SJSIP_{0.175\ m}$	312	285	119	439	0	275	410	1.91	590	10.6	4.1 ± 5.5
$SJSIP_{0.190\ m}$	309	274	130	427	0	276	420	1.9	600	9.9	6.3 ± 4.0
$SJSIP_{0.205\ m}$	248	275	177	265	0	252	590	2.65	570	5.1	4.1 ± 1.2
$SJSIP_{0.300\ m}$	289	404	98	401	0	252	580	2.74	560	3.6	2.8 ± 1.4

Values are presented for optimal stimulation onset times of muscles, time at which heel-off occurs (t_{ho}), knee angle at heel-off ($\varphi_{K,\,ho}$), duration of push-off (t_{total}), and maximum jump height ($z_{CM,\,max}$), mean jump height ($z_{CM,\,mean}$), and standard deviation in jump height distributions of 400 jumps in which stimulation onset times were perturbed with Gaussian noise (*SD* = 2 ms).

SJ: one-legged squat jump from the jumper's preferred initial position, with contact friction present, maximum stimulation of 0.5, and effective foot length of 16.5 cm. The stimulation onset times were found using height achieved by the center of mass as optimization criterion.

SJS: same as SJ, but initiated from the skater's position at the end of the gliding phase.

SJSI: same as SJS, but without contact friction.

$SJSIP_{0.165m}$: same as SJSI, but with a penalty on upper body rotation incorporated in the optimization criterion and an effective foot length of 16.5 cm.

$SJSIP_{0.175m}$ to $SJSIP_{0.300m}$: same as $SJSIP_{0.165m}$, but with effective foot lengths as indicated.

Muscles are soleus (SOL), gastrocnemius (GAS), vasti (VAS), rectus femoris (REC), gluteus maximus (GLU), and hamstrings (HAM).

a) friction removed without re-optimizing control
jump height: –0.18 m

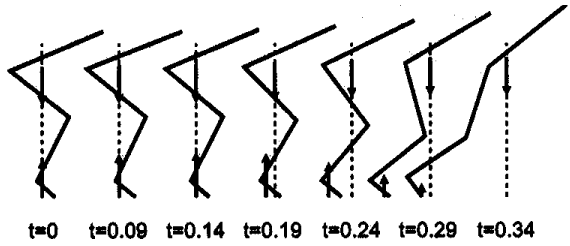

b) soleus erroneously switched on 50 ms earlier than optimal
jump height: 0.19 m

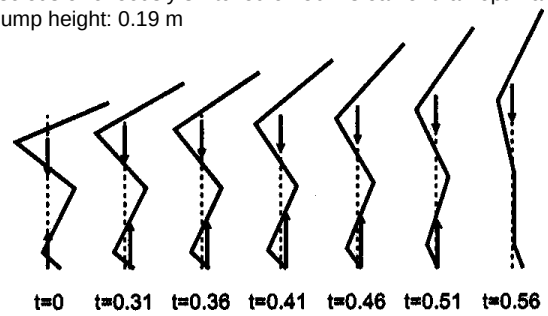

c) foot length increased without re-optimizing control
jump height: 0.04 m

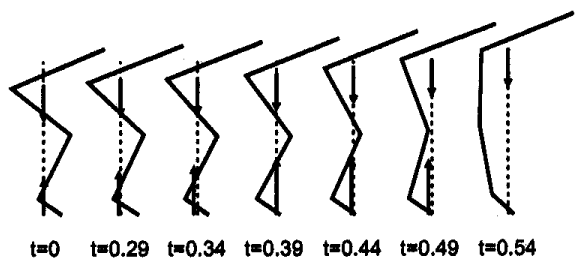

Figure 5 — Demonstration of effects of manipulating separate stimulation onset times or conditions. Setup of panels is as in Fig. 3. (a) Result obtained when optimal stimulation for the condition with contact friction was applied after removal of contact friction. (b) Result obtained when onset of soleus occurred 50 ms earlier than optimal. (c) Result obtained when optimal stimulation onset times for an effective foot length of 16.5 cm were applied to the initial equilibrium situation at an effective foot length of 19.0 cm.

When the set of stimulation onset times that was optimal for a simulated one-legged jump with normal friction present was applied to the model after removing surface friction, performance collapsed (Figure 5a). By reoptimization, however, jump height could be restored to 21 cm. In the new optimal solution, the angular displacement of the upper body was reduced and the whole leg rotated slowly backward in space during the push-off (Figure 4c). Moreover, jump height was more sensitive to variations in stimulation onset times (Table 1), indicating that the fitness landscape (jump height plotted in the space of stimulation onset times) was more rugged. Apparently, in the condition without surface friction, many combinations of small errors in stimulation onset times caused dramatic drops in jump height, due to breaking out of the foot either backward (see Figure 5a) or forward (Figure 5b).

The next step was to include a penalty on HATL rotation in the criterion and reoptimize the stimulation onset times. The reduction of HATL rotation was realized in the model (Figure 4d) primarily by switching on the hamstrings later (Table 1). The stimulation onset time of gluteus maximus was also changed, but this had little effect because the initial active state of this muscle was already high (see above). Due to the reduced hip extension, the hip muscles shortened less and produced less work during the push-off, causing maximum jump height to drop by 11.6 cm (Table 1).

When effective foot length was increased without reoptimization of stimulation onset times, performance again collapsed (Figure 5c). Maximum jump height at an effective foot length of 17.5 cm, obtained by reoptimization, was 1.2 cm greater than that at a length of 16.5 cm (Table 1). At effective foot lengths over 17.5 cm, maximum jump height decreased (Table 1). It dropped to 5.1 cm when effective foot length was increased from 17.5 cm to 20.5 cm, the value preferred by the skater. However, the average value of the distribution of heights in the perturbed jumps was 4.1 cm at both foot lengths, and at the length of 20.5 cm, jump height was least sensitive to errors in stimulation onset times (Table 1). When foot length was increased beyond 19.0, foot rotation started at progressively greater knee angles in the optimal solution (Table 1 and Figure 6).

Discussion

The purpose of the present study was to gain a better understanding of the mechanics of the push-off in speed skating by using an optimal control model developed for two-legged jumping, which was described and evaluated elsewhere (van Soest et al., 1993). The model was first adapted to one-legged jumping and evaluated by comparing its maximum-height jump (Figure 3b) with that of a human participant (Figure 3a). From the good correspondence in movement pattern and performance, we concluded that the model also represented the salient characteristics of the real system for one-legged jumping. Subsequently, we showed that the model's movement pattern was not dependent on the intensity of effort. Lowering the maximal stimulation of the muscles in the model from 1.0 to 0.5, and reoptimizing the stimulation onset times, produced a slow-motion version of the maximum jump, with height reduced by 1.7 cm (compare Figures 4a and 3b). Starting from this slow-motion one-legged jump, we studied how performance was affected, by: (a) changing the starting position from that in jumping to that in speed skating; (b) reducing

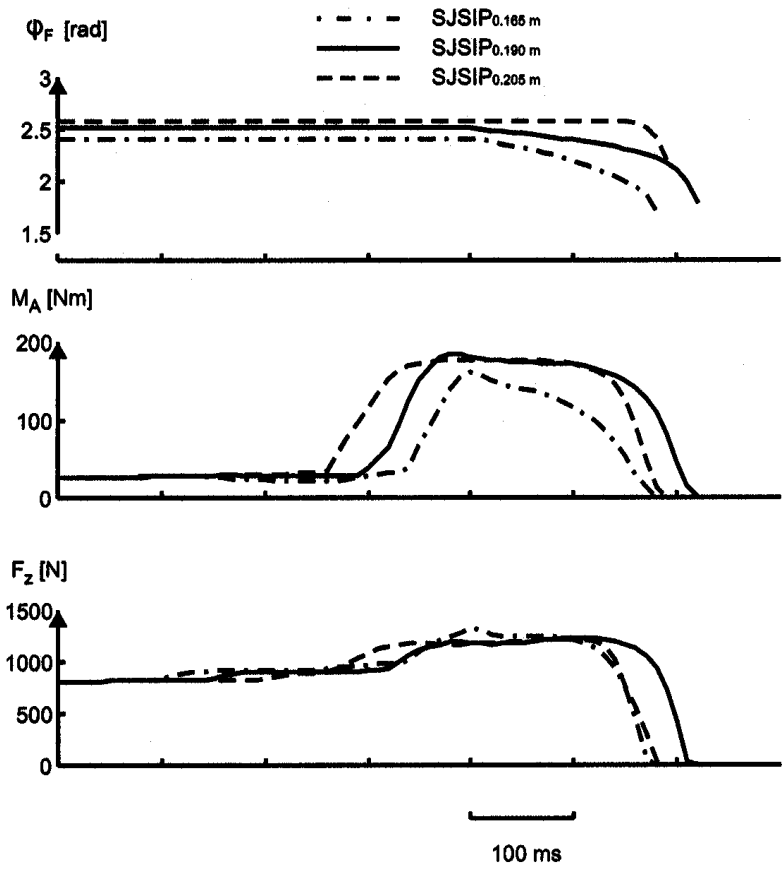

Figure 6 — Time histories of foot angle (see definition in Fig. 1), plantar flexion moment (M_A), and vertical ground reaction force (F_z) for optimal solutions at effective foot lengths of 16.5 cm, 19 cm, and 20.5 cm. The solutions pertain to the condition in which no contact friction was present and a penalty on upper body rotation was incorporated in the optimization criterion.

the friction between foot and ground to zero; (c) introducing the requirement to maintain the upper body in a more or less horizontal position; and (d) increasing the effective foot length from natural values to values operative in speed skating. These manipulations turned out to affect maximum height as well as the robustness of performance. Below we shall elaborate the insights gained by the simulations and then discuss whether the simulation results help us understand observations made in experimental studies of speed skating.

When the initial position of the model was changed to that of the skater at the end of the gliding phase (Figure 4b), vasti and hip extensors were switched on

earlier in the optimal solution, and plantar flexors later (Table 1). These adaptations can be understood if we realize that relative to the toes, the center of mass lies more backward in the skater's starting position than in the jumper's starting position (compare Figures 4b and 4a). To achieve a maximum performance, the model must realize a greater forward displacement of the center of mass during the push-off, and this requires that the stimulation onset of the plantar flexors be delayed relative to that of the hip extensors (Bobbert & van Zandwijk, 1999a). Because the more crouched position allowed the muscles to shorten further during the push-off, they could produce more work, and maximum jump height increased from 21.0 to 22.2 cm (Table 1).

When friction between foot and ground was reduced to zero, maximum jump height dropped by 1.2 cm and performance became more sensitive to errors in stimulation onset times (Table 1). This can be understood as follows: With normal friction, errors in stimulation onset times tend to cause aberrations in the acceleration of the center of mass. By contrast, when friction is zero, the center of mass has a fixed horizontal position, and errors in stimulation onset times tend to cause aberrations in the acceleration of the relatively light leg segments, and hence accelerations of the foot relative to the ground. Because the mass involved is much smaller in the latter case, the aberrations in foot motion are bigger. Furthermore, displacements of the foot are hazardous because they tend to be regenerative. That is, they tend to increase the transfer from muscle forces to foot accelerations in the direction of the displacement. This positive feedback could eventually cause the foot to break out (Figure 5a and 5b). Thus, when friction was reduced to zero, the tolerance to errors in stimulation onset times decreased (Table 1).

The reduction of maximum jump height, which occurred when surface friction was reduced to zero, implies that the solution space is constrained without friction. The reason seems to be that taking away friction introduces the need to control the accelerations of the foot. To explain this, we must take into account the actions of the individual muscles. In the jump with normal friction, activation of the hamstrings caused a forward acceleration of the center of mass (note the initial forward surge of the ground reaction force in Figure 4b). The action of the hamstrings remained unopposed until soleus was activated 268 ms later (Table 1), which caused the acceleration of the center of mass to change from forward to backward some 250 ms before takeoff (Figure 4b). In the jump without friction, the action of the hamstrings gives the foot a large backward acceleration. When left unopposed for too long, it would cause the foot to break out backward (Figure 5a). To prevent this, gastrocnemius was activated (Table 1). Because this bi-articular muscle not only increases the plantar flexion moment but also reduces the knee extension moment, the transfer of its force to forward acceleration of the foot is smaller than that of soleus. Switching on the soleus too early would cause the foot to break out forward (Figure 5b). Hence it was delayed until the foot had been displaced further backward, so that the transfer of its force to forward acceleration of the foot was smaller. As a matter of fact, the backward shift of the foot seems to serve the very purpose of decreasing the latter transfer, and concomitantly increasing the transfer to vertical acceleration of the center of mass.

Introducing the requirement to maintain the upper body in a more or less horizontal position caused a decrease of maximum jump height by 11.6 cm (Table 1). The requirement was satisfied primarily by late activation of the bi-articular

hamstrings, which reduced the anticlockwise rotation of the upper body via two mechanisms. First, the hamstrings did not contribute to the extension moment at the hip during the first part of the push-off, and thus did not contribute to anticlockwise acceleration of the upper body. Second, the hamstrings no longer opposed the extension moment of the vasti during the first part of the push-off. This allowed for a greater angular acceleration at the knee and a concomitant greater upward acceleration of the hip, which tends to cause a clockwise angular acceleration of the upper body (Bobbert & van Soest, 2001). The limitation of angular displacement of the upper body caused a limitation of the shortening distance of hamstrings and gluteus maximus, and hence an inevitable reduction of work output of these muscles. The reduction in work output of these muscles was the main reason for the decrease in maximum jump height.

Increasing effective foot length influenced several variables related to performance. The greatest effect occurred when foot length was increased from 19 cm to 20.5 cm: maximum jump height dropped by 4.8 cm, but performance became more robust (Table 1). At foot lengths of 20.5 cm and beyond, the increases in angular velocities of foot and leg segments became de-synchronized. As a result, the peak vertical velocity of the center of mass was lower, even though the angular velocities in the joints were higher (Figure 7). The explanation lies in the geometrical transfer from angular velocities of segments to vertical velocity of the center of mass (Bobbert & van Ingen Schenau, 1988). The cause of the desynchronization is the delayed start of foot rotation at a foot length of 20.5 cm. The delay was not due to a delay in stimulation onset of the plantar flexors; in the optimal solution at a foot length of 20.5 cm, soleus was actually activated earlier than at smaller foot lengths (Table 1).

The explanation for the delayed start of foot rotation is purely mechanical. Two reaction forces act on the foot: the ground reaction force and the joint reaction force at the ankle. As long as the acceleration of the foot is zero, the difference between these two forces is the weight of the foot, which is negligible. Thus, to a first approximation, the two forces are equal in magnitude but opposite in direction; the joint reaction force is pointing vertically downward and the ground reaction force is pointing vertically upward (vertically, because there is no friction). When the plantar flexion moment is zero, their lines of action coincide and run through the ankle joint. When the plantar flexion moment is increased while the moments at the knee and hip joints remain the same, the reaction forces increase in magnitude and the line of action of the ground reaction force moves away from the ankle joint toward the toes so that it now forms a couple with the reaction force at the ankle. As long as the heel remains on the ground, this couple is equal in magnitude but opposite in direction to the plantar flexion moment. Foot rotation does not start until the line of action of the ground reaction force has reached the axis of rotation. All else being equal, the plantar flexion moment required to initiate foot rotation becomes greater when foot length is increased. Thus, rotation of the foot is expected to start later because it requires a further buildup of plantar flexion moment. When foot length becomes so large that even the maximum value of the plantar flexion moment is insufficient to push the center of pressure to the axis of rotation, heel lift does not occur until the acceleration of the center of gravity—and therewith the couple of the reaction forces—decreases. We can now understand why the foot starts to rotate so late at the effective foot length of 20.5 cm: the

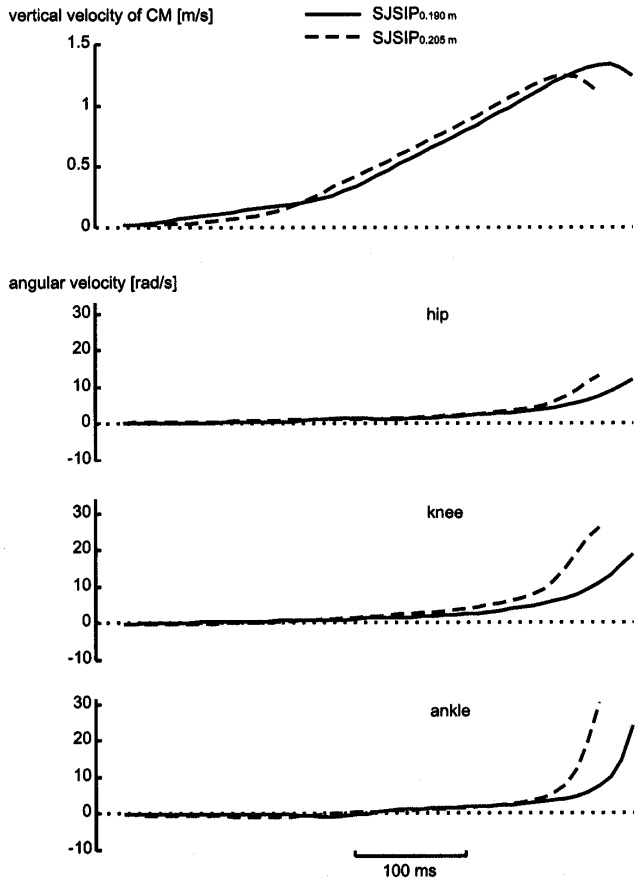

Figure 7 — Time histories of joint angular velocities (see joint angle definition in Fig. 2) and vertical velocity of the center of mass for optimal solutions at effective foot lengths of 19 cm and 20.5 cm. The solutions pertain to the condition in which no contact friction was present and a penalty on upper body rotation was incorporated in the optimization criterion.

maximum plantar flexion moment is insufficient to initiate an early rotation of the foot, so this rotation is delayed until the knee and hip joint moments decrease and the reaction force drops to some 700 N.

Meanwhile the knee angle has increased to 152° (2.65 rad, Table 1). Note in Figure 4f that the knee is hyperextended at takeoff (there were no passive constraints in the model). This means that before takeoff, the distance from hip to ankle has already started to decrease. Because the leg as a whole was rotating, however, the vertical distance between the hip joint and the tip of the skate was still increasing, and the model could still push against the ground. It is clear that

this required a net knee flexion moment (the knee joint moment is dominated by the flexor moments of hamstrings and gastrocnemius). Since the knee continued to entend, energy was being absorbed at the knee during the last 50 ms of the push-off.

The behavior of the foot and the concomitant de-synchronization of segment angular velocities help us understand why maximum jump height dropped 4.8 cm when foot length was increased from 19 to 20.5 cm. The drop in maximum jump height was related to a 40-J decrease in total work produced. Total work decreased because five of the six muscles in the model generated less work; only the rectus femoris generated 4 J more. Muscle work is the integral of muscle force with respect to shortening distance. It was reduced primarily because the monoarticular muscles shortened at a higher speed, and hence suffered more from their force-velocity relationship. This in turn was due to the higher angular velocities of the joints at the effective foot length of 20.5 cm (Figure 7). Remember that the higher joint angular velocities did not produce a higher vertical velocity of the center of mass (Figure 7).

The behavior of the foot also helps us understand why robustness of performance increased when foot length was increased from 19 to 20.5 cm. In a previous study (Bobbert & van Zandwijk, 1999b) it was argued that when the heel is off the support surface, errors in stimulation onset times of the plantar flexors cause regenerative aberrations in the configuration of the system. This problem is magnified when the friction between foot and ground is reduced to zero (Table 1). At a foot length of 20.5 cm or more, the heel remains on the ground until the very end of the push-off, so it is not surprising that the movement was most robust in this condition.

Does the insight gained by the simulations improve our understanding of the mechanics of the push-off in speed skating? Results similar to those found in the simulation study were obtained in an experimental study, in which the hinge of the klapskate was manipulated (Houdijk et al., 2001). When the hinge was located anteriorly, the onset of foot rotation occurred later, the angular displacement and peak angular velocity of the knee were greater, the net knee flexion moment at the end of the push-off was larger, and work produced at the knee was smaller than when the hinge was located posteriorly. Similar differences were found when skating with conventional skates, with an effective foot length of about 30 cm, compared to skating with klapskates (Houdijk et al., 2000). According to the simulation results, the explanation lies in the effect of foot length on the interplay between the plantar flexion moment and the couple of the reaction forces acting on the foot, as explained above.

Interestingly, in the simulation model, the greatest performance could be reached at an effective foot length of 17.5 cm (Table 1). This raises the question of why speed skaters do not choose to have the hinge of the klapskates closer to the ankle. From subjective reports of skaters participating in a study on the effects of changing the location of the hinge (Houdijk et al., 2001), we have learned that this "does not feel right." Based on the simulation results, it is tempting to speculate that moving the axis closer to the ankle would increase the maximum performance (Table 1), but it would also make the performance less robust (Table 1). Obviously, it is of no use to have a greater theoretical maximum performance if the chances of actually achieving it are very small due to noise in the control signals (Bobbert & van Zandwijk, 1999). In that case, it is better to have a more robust

performance, which is achieved at greater effective foot lengths (Table 1). Since robustness is greatly reduced by removing surface friction, it may not be safe to assume, as was done elsewhere (Allinger & Motl, 2000), that jumping from the ground is a suitable method for testing skates.

All in all, the simulations performed in this study have helped us gain a better understanding of push-off mechanics in speed skating. In particular, the role of surface friction and effective foot length have been clarified. However, a number of differences remain between the simulation results and the data on speed skating (Figures 4e, 4f, and 3c, respectively). For instance, in the simulations with the effective foot length of the skater (20.5 cm), the knee was hyperextended at takeoff. In a real system, of course, there is an anatomical constraint (van Ingen Schenau et al., 1987). Perhaps in order to satisfy this constraint, the skater made a small countermovement (see Figure 3c) by temporarily reducing the plantar flexion moment and hence the extension moment acting on the shank. In the simulation model this could not be reproduced, of course, because the muscles were only allowed to increase their stimulation. Furthermore, the simulation study neglects a number of potentially important factors, such as the swinging and subsequent weight-bearing of the contralateral leg (the foot of this leg is already on the ice during the final 100–150 ms of the push-off), and the rotation of the skater in the frontal plane, which changes the effects of the gravitational force. Future simulation studies might clarify the importance of these factors and provide further insight into the relationship between the optimal location of the hinge of the skate and, for instance, segment lengths and strength of plantar flexors relative to that of knee and hip extensors.

References

Allinger, T.L., & Motl, R.W. (2000). Experimental vertical jump model used to evaluate the pivot location in klap speed skates. *Journal of Applied Biomechanics*, **16**, 142-146.

Allinger, T.L., & van den Bogert, A.J. (1997). Skating technique for the straights, based on the optimization of a simulation model. *Medicine and Science in Sports and Exercise*, **29**, 279-286.

Bobbert, M.F., & van Ingen Schenau, G.J. (1988). Coordination in vertical jumping. *Journal of Biomechanics*, **21**, 249-262.

Bobbert, M.F., & van Soest, A.J. (2001). Why do people jump the way they do? *Exercise and Sport Sciences Reviews*, **29**, 95-102.

Bobbert, M.F., & van Zandwijk, J.P. (1999a). Dynamics of force and muscle stimulation in human vertical jumping. *Medicine and Science in Sports and Exercise*, **31**, 303-310.

Bobbert, M.F., & van Zandwijk, J.P. (1999b). Sensitivity of vertical jumping performance to changes in muscle stimulation onset times: A simulation study. *Biological Cybernetics*, **81**, 101-108.

de Boer, R.W., Cabri, J., Vaes, W., Clarijs, J.P., Hollander, A.P., de Groot, G., & van Ingen Schenau, G.J. (1987). Moments of force, power, and muscle coordination in speed-skating. *International Journal of Sports Medicine*, **8**, 371-378.

Hatze, H. (1981). *Myocybernetic control models of skeletal muscle characteristics and applications*. Pretoria: University of South Africa.

Houdijk, H., de Koning, J.J., Bobbert, M.F., & de Groot, G. (2001). The effect of the foot's center of rotation on push-off mechanics in speed skating. In H. Houdijk, *The klapskate, shifting gears in speed skating* (pp. 75-90). Amsterdam: Vrije Universiteit.

Houdijk, H., de Koning, J.J., de Groot, G., Bobbert, M.F., & van Ingen Schenau, G.J. (2000). Push-off mechanics in speed skating with conventional skates and klapskates. *Medicine and Science in Sports and Exercise*, **32**, 635-641.

Pandy, M.G., Zajac, F.E., Sim, E., & Levine, W.S. (1990). An optimal control model for maximum-height human jumping. *Journal of Biomechanics*, **23**, 1185-1198.

van Ingen Schenau, G.J. (1982). The influence of air friction in speed skating. *Journal of Biomechanics*, **15**, 449-458.

van Ingen Schenau, G.J. (1989). From rotation to translation—Constraints on multi-joint movements and the unique action of bi-articular muscles. *Human Movement Science*, **8**, 301-337.

van Ingen Schenau, G.J., & Bakker, K. (1980). A biomechanical model of speed skating. *Journal of Human Movement Studies*, **6**, 1-18.

van Ingen Schenau, G.J., Bobbert, M.F., & Rozendal, R.H. (1987). The unique action of bi-articular muscles in complex movements. *Journal of Anatomy*, **155**, 1-5.

van Ingen Schenau, G.J., de Groot, G., Scheurs, A.W., Meester, H., & de Koning, J.J. (1996). A new skate allowing powerful plantar flexions improves performance. *Medicine and Science in Sports and Exercise*, **28**, 531-535.

van Soest, A.J., & Bobbert, M.F. (1993). The contribution of muscle properties in the control of explosive movements. *Biological Cybernetics*, **69**, 195-204.

van Soest, A.J., & Casius, L.J.R. (in press). The merits of parallelization in solving hard optimization problems. *Journal of Biomechanical Engineering*.

van Soest, A.J., Schwab, A.L., Bobbert, M.F., & van Ingen Schenau, G.J. (1993). The influence of the biarticularity of the gastrocnemius muscle on vertical-jumping achievement. *Journal of Biomechanics*, **26**, 1-8.

van Zandwijk, J.P., Bobbert, M.F., Baan, G.C., & Huijing, P.A. (1996). From twitch to tetanus: Performance of excitation dynamics optimized for a twitch in predicting tetanic muscle forces. *Biological Cybernetics*, **75**, 409-417.

Zajac, F.E., & Gordon, M.E. (1989). Determining muscle's force and action in multi-articular movement. *Exercise and Sport Sciences Reviews*, **17**, 187-230.

Acknowledgments

The authors gratefully acknowledge the help of Dr. I. Kingma in collecting the data on jumping. The work of H. Houdijk was supported by the Technology Foundation STW, Applied Science Division of NWO, and the Technology Programme of the Ministry of Economic Affairs.